IEEE Access
Multidisciplinary | Rapid Review | Open Access Journal

Received August 21, 2018, accepted September 28, 2018, date of publication October 17, 2018, date of current version November 9, 2018.

Digital Object Identifier 10.1109/ACCESS.2018.2875359

A Ka-Band High-Efficiency Transparent Reflectarray Antenna Integrated With Solar Cells

WENXING AN[1], LIN XIONG[2], SHENHENG XU[2], (Member, IEEE), FAN YANG[2], (Senior Member, IEEE), HAI-PENG FU[1,4], (Member, IEEE), AND JIAN-GUO MA[3,4], (Fellow, IEEE)

[1]Tianjin Key Laboratory of Imaging and Sensing Microelectronic Technology, School of Microelectronics, Tianjin University, Tianjin 300072, China
[2]Department of Electronic Engineering, Tsinghua University, Beijing 100084, China
[3]School of Computer, Guangdong University of Technology, Guangzhou 510006, China
[4]Qingdao Key/Engineering Laboratory of Marine Information Perception and Transmission, Tianjin Engineering Center of Integrated Circuit and Computing Systems, Tianjin International Joint Research Center of Internet of Things, Tianjin University, Tianjin 300072, China

Corresponding author: Hai-Peng Fu (hpfu@tju.edu.cn)

This work was supported in part by the National Key Research and Development Program of China (Nano Science and Technology Project) under Grant 2016YFA0202200, in part by the National Natural Science Foundation of China under Grant 61701339, and in part by the AoShan Talents Cultivation Program Supported by the Qingdao National Laboratory for Marine Science and Technology under Grant 2017ASTCP-OS03.

ABSTRACT A transparent reflectarray antenna integrated with solar cells is presented for satellite communications in the paper. The electromagnetic characteristics of solar cells at *Ka*-band are investigated, and a sub-wavelength X-shaped dipole element is designed to augment the reflectarray's performance. A prototype with an aperture of 160 × 150 mm^2 is then analyzed, fabricated, and tested to validate the proposed design. The simulation and measurement results show good radiation characteristics, and the measured gain at 20 GHz is 27.3 dBi with an aperture efficiency of 40.0%. Low side-lobe and cross polarization levels are obtained. Furthermore, the solar energy efficiency of the proposed transparent reflectarray antenna is studied through an optical blockage experiment. The optical blockage ratio is less than 9.9% and at least 81% of light transmittance has been achieved. This work continues to propel the research on reflectarray antennas integrated with solar cells, making it more promising for practical applications in space satellite communications.

INDEX TERMS Antenna, integration, satellite communication, reflectarray, solar cell.

I. INTRODUCTION

Space exploration has attracted global attentions recently. For large-scale commercial applications, it is necessary to control the overall cost. The launching cost has been reduced effectively after the success of Falcon Heavy rocket from SpaceX. To further decrease the cost, some other technologies have to be considered.

In order to augment the data transfer rate at space, the high gain antenna has been developed with large aperture and volume, such as reflector antennas. Due to the limited volume and mass on small satellites, a compact and lightweight high-gain antenna with good radiation performance is much preferred. To meet the stringent demands with limited space, an effective way is to integrate together multiple functional devices for different applications. As the solar panel can offer a large planar area for solar energy harvesting, it is potential to integrate high-gain antennas with solar panels.

The concept of solar antennas was proposed since 1990's and different types of solar antennas have been studied, such as the conventional meshed and transparent patch [1]–[4], monopole [5], dipole [6], PIFA [7]–[9], slot [10]–[12], DRA [13], [14], Vivaldi [15], and metasurface loaded antenna [16]. A wearable textile antenna based on substrate integrated waveguide was presented in [17]. However, these aforementioned designs can only achieve relatively low gains. A medium gain antenna array was discussed in [18] based on L-probe fed elements. In order to obtain a high-gain antenna for long-distance satellite communications, the

reflectarray antenna integrated with solar cells was first proposed in [19]–[21] using cross dipole elements with an aperture efficiency of approximately 10%.

Since 2012 NASA/JPL has initiated the ISARA project [22], integrating a Ka-band reflectarray antenna with the solar panel of the cubesat. Then, many efforts have been made to improve the reflectarray's radiation performance. Two types of elements were studied in [23] that can be integrated on top of solar cells for small satellite application. An improved design with cross dipoles introduced in [24] achieved good radiation characteristics. The measured gain of 26.3 dBi was realized with an aperture efficiency of 29.8%, and the optical blockage ratio was 17.6%. In order to reduce the optical blockage, a high-gain conformal cubesat reflectarray antenna was presented in [25]–[27] with overall transparency of more than 90%, while the simulated aperture efficiency was 45%. Instead of metallic material, a transparent element design was presented in [28] using a transparent conductive patch on a glass substrate, but there was no discussion on the antenna performance. Furthermore, transparent reflectarray using indium tin oxide was proposed for linear polarization applications in [29] with the measured gain of 22.8 dBi. An aperture efficiency of 44.3% with 100% optical transparency was realized based on the ITO material and PEC ground. Based on the solar cell substrate, an optically transparent lens was realized in [30]. This novel design manipulated the element dielectric constant by drilling variable air holes in transparent dielectric materials to achieve certain aperture reflected phase distribution. It can provide the minimum optical blockage with an aperture efficiency of 25%; however, the structure was relatively bulky for space applications. To sum up, solar reflectarrays with higher aperture efficiency and lower optical blockage ratio are much preferred for future space applications.

In this paper, a Ka-band reflectarray integrated with solar cells is presented to achieve better antenna and optical performances. A sub-wavelength X-shaped dipole element is adopted to augment reflectarray's performance, which is experimentally verified by measurements of a prototype. Compared with previous designs, the measured aperture efficiency is successfully increased to be 40.0%, while the optical blockage ratio is decreased to be 9.9%.

II. PROPOSED ELEMENT STRUCTURE INTEGRATED WITH SOLAR CELLS

As the solar cell serves as an essential integrated part of the substrate of a solar reflectarray, it is critical to assess its electromagnetic characteristics at the frequency band of interest. Then, the element structure is designed and its performance is analyzed.

A. MULTILAYER STRUCTURE OF SOLAR CELLS

A specific type of solar cells is shown in Fig. 1(a) with a rectangular size of 40 × 30 mm^2 and a truncated corner. The multilayer structure of the solar cell is depicted in Fig. 1(b), which is similar to that in [24] except for the glass glue.

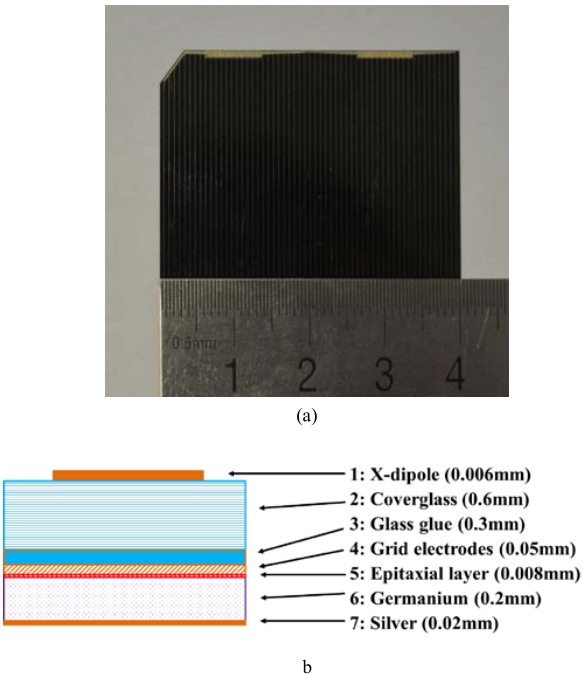

FIGURE 1. The solar cell and its structure: (a) photograph of a solar cell. (b) the multilayer structure of the solar cell with integrated reflectarray elements (X-dipoles).

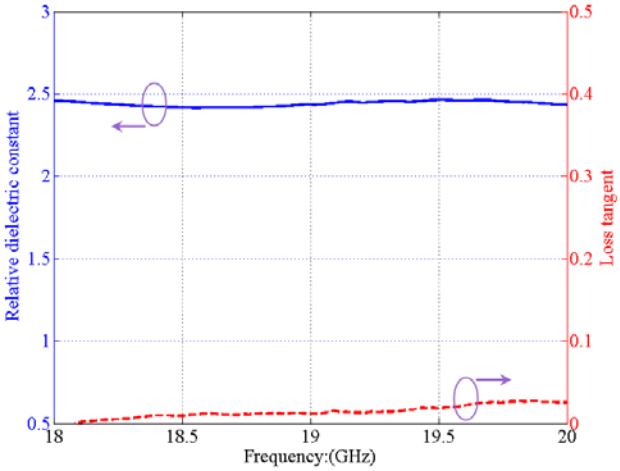

FIGURE 2. Measured glass glue's relative dielectric constant and loss tangent.

The electromagnetic parameters of the adopted glass glue are measured using a standard waveguide method and a network analyzer. It is shown in Fig. 2 that at the design frequency of 20 GHz, the measured relative dielectric constant is 2.43 with the loss tangent of 0.0255, which remain stable in the Ka band. The measured relative dielectric constant of the cover glass is 6.39 and the loss tangent is 0.0135 at 20 GHz.

The conductivities of epitaxial layer and doped germanium are 2.6×10^5 S/m and 2.3×10^3 S/m at DC, respectively. For a non-ideal conductor, its conductivity is frequency dependent at AC, which can be calculated according to the following

formula from the Drude model:

$$\sigma = \frac{n_e e^2}{m_e(\gamma_0 + j\omega)} = \frac{\sigma_0}{(1 + j\frac{\omega}{\gamma_0})} \tag{1}$$

where n_e is the carrier concentration and γ_0 is the reciprocal of relaxation coefficient, which can be measured through the Hall effect experiment; e is electron charge and m_e is electron mass; ω is the angular frequency, which equals $2\pi f$. σ_0 is the conductivity at DC. Based on these frequency independent parameters and ω, the imaginary part of the epitaxial layer is calculated to be only ∼5% of the real part at 20 GHz, and its influence will be discussed in the following section.

B. ELEMENT DESIGN

A novel X-shaped metallic dipole with a width of 0.2 mm is chosen as the phasing element, shown in Fig. 3, which is printed directly on the cover glass. The proposed element is simulated in a periodic environment, and its simulated element phase and magnitude responses are shown in Fig. 4. For comparison, the performances of the cross dipole element are also plotted in Fig. 4 with the same configuration.

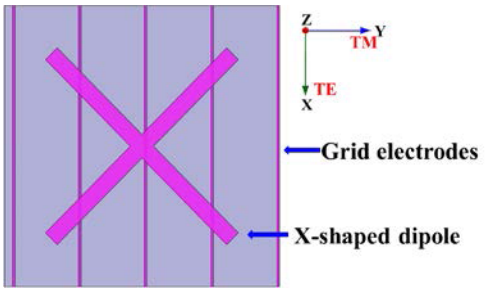

FIGURE 3. Top view of the X-shaped dipole element.

It is observed that two elements have similar phase range. However, the X-shaped dipole can make full use of the corners of the unit space and the dipole length can have a larger variation. Consequently, the X-shaped dipole has a gentler phase curve, and hence, the phase error caused by fabrication errors and the variation in material properties of the solar cells can be reduced effectively.

Based on the proposed X-shape element, the unit size can be reduced to 3.33 mm ($0.22\lambda_0$ at 20 GHz), which is even smaller than that in [24]. The sub-wavelength structure can mitigate the influence of highly lossy substrate (solar cells) on the element magnitude performance [31]. The introduced glass glue layer can also contribute to reduce the magnitude loss, because a thicker substrate can result in less magnitude loss [32]. Based on the sub-wavelength unit and glass glue structure, it is observed from Fig. 4 that the magnitude loss is reduced to 1.4 dB, exhibiting a great improvement compared with that in [24].

As previously mentioned, the imaginary part of the conductivity of the epitaxial layer is calculated at 20 GHz, which would cause potential influence on the element performance, so it is necessary to quantify these effects. Fig. 5 shows the

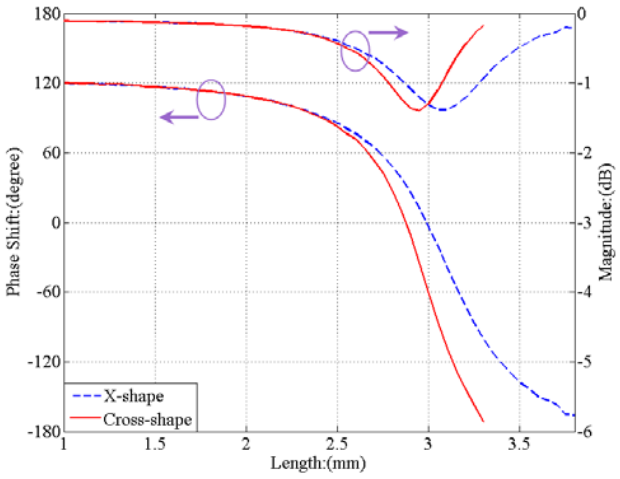

FIGURE 4. Simulated element performances of the X-shaped and cross dipoles.

element performances with and without the imaginary part of conductivity of the epitaxial layer. It is clear that the phase curves for both cases almost overlap with each other, while the magnitude curves have a difference of 0.05 dB due to the effect of the imaginary part. Therefore, the effect caused by the imaginary part of conductivity can be neglected.

For dual-linear polarization, it is necessary to investigate the influence of asymmetric grid electrodes under the illumination of different polarization source. Fig. 6 shows the element performances with TE and TM source. It is observed that two phase curves almost overlap with each other, the maximum deviation between two magnitude curves is only 0.02 dB with the dipole length of 3.1 mm. Based on the simulation results, it can be concluded that the grid electrodes have little influence on the element performance, no matter TE or TM source.

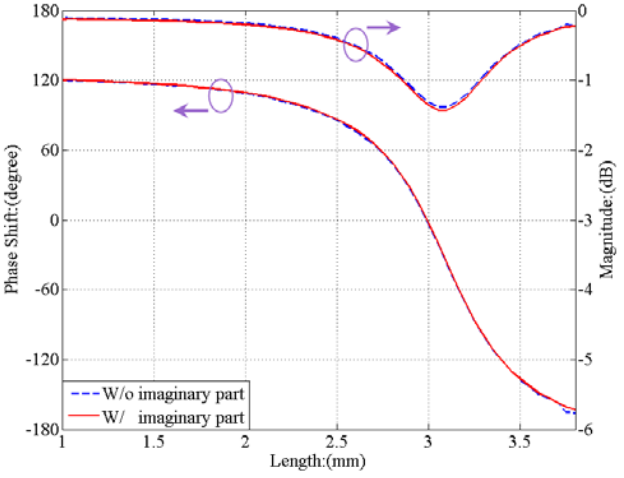

FIGURE 5. Simulated element performance with and without the imaginary part of conductivity of the epitaxial layer at 20 GHz.

The oblique incidence performances of the proposed element are discussed in Fig. 7. The oblique incident angle is

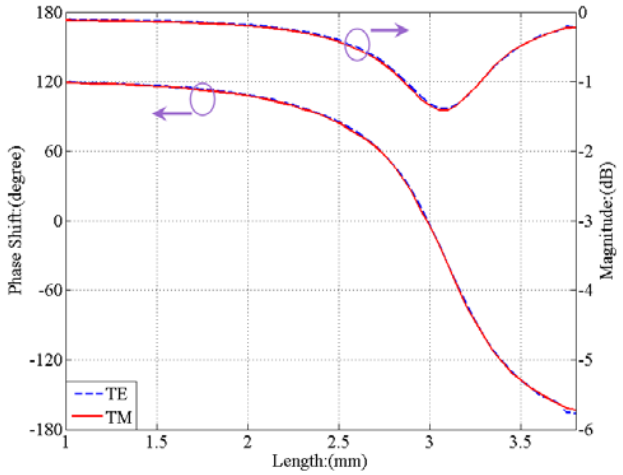

FIGURE 6. Simulated element performances with TE and TM sources.

set as 45° for the TE/TM source. The phase and magnitude curves are plotted in Figs. 7(a) and 7(b), respectively. Compared with the element performance under normal incidence, it is observed that the maximum phase deviation between them is 43°, while the maximum magnitude deviation is 0.5 dB. For most elements, the oblique direction is less than 45°, so the potential phase error and magnitude loss are much less.

To sum up, the element analysis can provide some guidelines for future designs. The X-shaped dipole can offer more tolerance of phase errors from fabrication, assembly and variation in material properties of the solar cells, the magnitude loss is also mitigated by introducing sub-wavelength element and thick substrate, thus greatly enhancing its potential for space applications. At 20 GHz, the imaginary part of conductivity has little influences on the element performance, so the conductivity at DC can be directly used for quick evaluation of the element's performance. The element performance is less sensitive to the asymmetric structure of grid electrodes, making it promising for dual-linear and circular polarization. The phase and magnitude differences between normal and oblique incidence are still acceptable for engineering applications. With the glass glue layer, the element's multilayer structure, except the additional metallic dipoles, is the same as that of the solar cells in production, and hence, the proposed design is more suitable for future practical applications.

III. PROTOTYPE DESIGN AND EXPERIMENTAL RESULTS

In order to validate the proposed element structure, a reflectarray prototype integrated with solar cells at 20 GHz is designed, fabricated, and measured.

A. REFLECTARRAY CONFIGURATION

The reflectarray prototype is shown in Fig. 8 with an aperture size of $160 \times 150\ \text{mm}^2$. 20 solar cells as shown in Fig. 1(a) are utilized as the reflectarray substrate, with copper foils filling the corners between the solar cells.

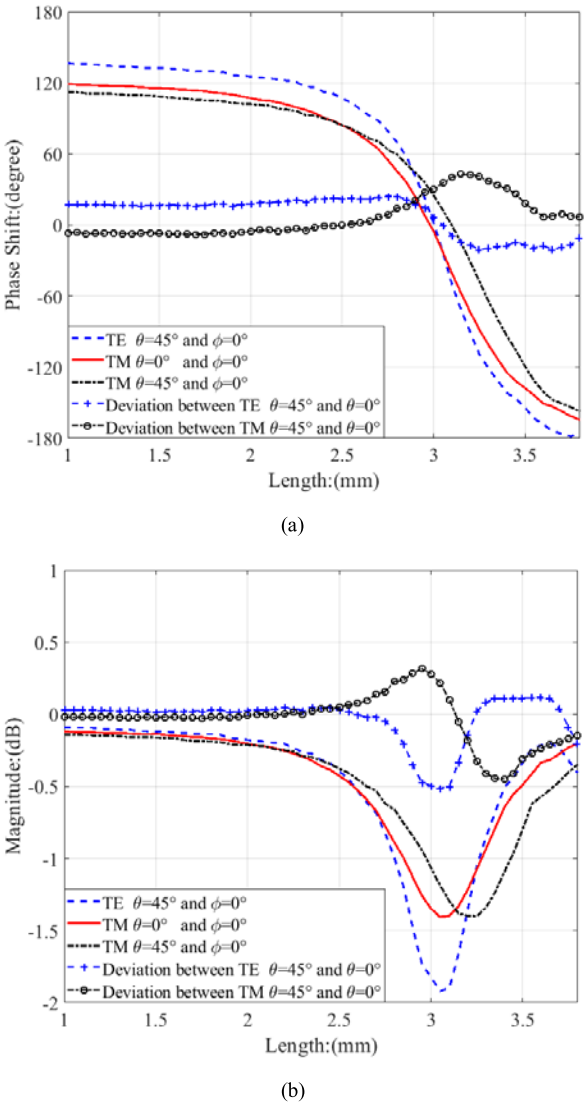

FIGURE 7. Simulated element performances with oblique incidence: (a) phase, (b) magnitude.

A vertically polarized corrugated horn with a gain of 16.3 dBi is employed as the primary feed. A simple $\cos^q(\theta)$ function without azimuth dependence is utilized to model the feed's radiation pattern, and the corresponding q factor is 10.2. To reduce the feed blockage, the horn is placed 155 mm above the aperture with an oblique illumination angle of 15°. The main beam direction of reflectarray is also 15° off the broadside of the aperture.

The reflectarray aperture consists of a total number of 2112 X-dipole elements. The required phase of each element is then calculated using the ray tracing method to compensate the spatial path delay from the feed and collimate the main beam in the predefined direction. The calculated phase distribution is plotted in Fig. 9(a). The magnitude distribution of the aperture can be determined by considering the magnitude and path loss of each element. It is observed that the edge taper is about −10 dB, which is helpful to realize a higher aperture efficiency. Note that the optical blockage

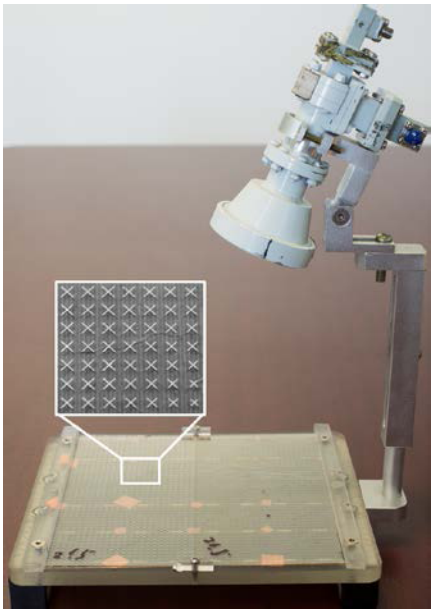

FIGURE 8. Photo of the fabricated reflectarray prototype.

is taken into account and is marked by the shadowed area in Fig. 9(b).

Because the X-dipole elements are made of metallic materials, the light in the X-dipole area is blocked. However, due to the narrow dipole width of 0.2 mm, the total area of the metallic dipoles is calculated to be only 9.9% of the entire aperture area. The optical blockage ratio is relatively small, and its influence on the solar cell's performance is very limited. Hence, the designed solar reflectarray can be considered as a transparent antenna.

B. SIMULATION AND EXPERIMENTAL RESULTS

Based on the aperture phase and magnitude distributions, the radiation performance of the proposed reflectarray is calculated using the array theory method [33]. The calculated radiation pattern is shown in Fig. 10, where the calculated gain at 20 GHz is 28.4 dBi and the aperture efficiency is 56.6%.

The reflectarray prototype is measured in an anechoic chamber, and the measured radiation pattern is also plotted in Fig. 10. The measured main beam is in good agreement with the simulation. The measured first side-lobe and cross-polarization levels are −17.0 dB and −26.8 dB, respectively. The tested gains within the frequency band of interest are shown in Fig. 11, which is 27.3 dBi at 20 GHz, corresponding to an aperture efficiency of 40.0%. Due to the subwavelength element spacing and the gentle phase curve of the X-shaped dipole element, the measured 1-dB gain bandwidth is 12.9%. Certain discrepancies between the calculated and measured results are observed, which are mainly due to the following factors:

1. As some elements on the aperture are illuminated obliquely by the feed. For convenience, the magnitude and phase curves under normal incidence are adopted for reflectarray design, so there will be certain amplitude errors with the maximum value of 43° and phase errors with the maximum value of 0.5 dB for these cells under oblique illumination;

2. Due to the imperfect fabrication process, certain X-shaped elements are not printed correctly. The incomplete elements will cause certain amplitude and phase errors. Taking this into account, the simulation results show that the first side-lobe level has increased 1 dB;

3. At the assembly process, the air gaps are inevitable during the procedure of assembling the cover glass, glass glue and solar cells together. The air gaps also exist between different solar cells. These air gaps would cause certain phase and magnitude errors. Additionally, the EM-waves are sensitive to the metallic mounting frame for test configuration, which would cause certain pattern deterioration;

4. The back radiations of the reflectarray are not considered in calculations using the array theory method, which would cause higher side-lobe levels.

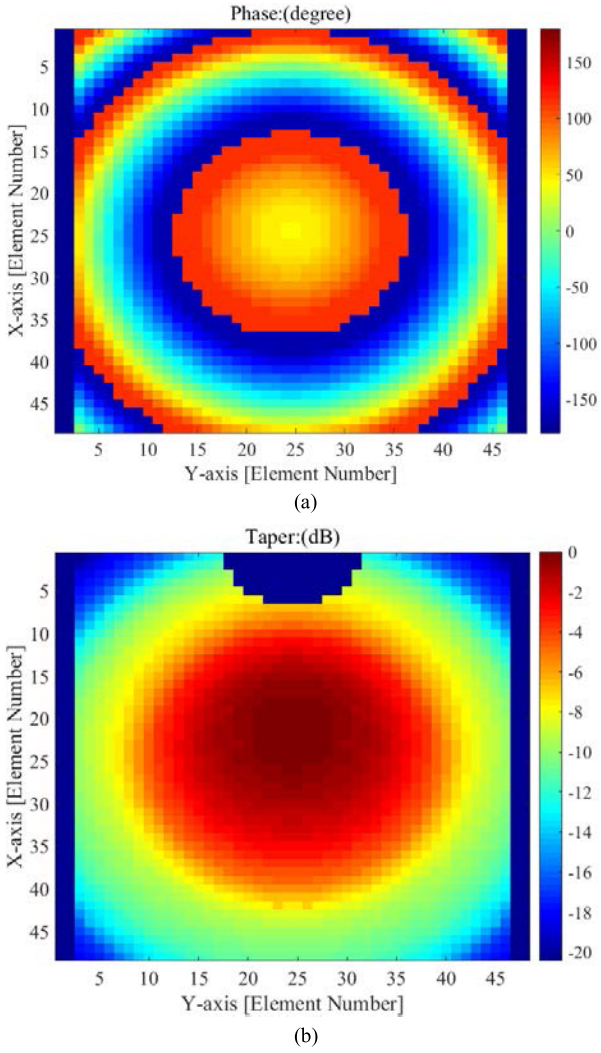

FIGURE 9. Calculated aperture distributions: (a) phase, (b) magnitude.

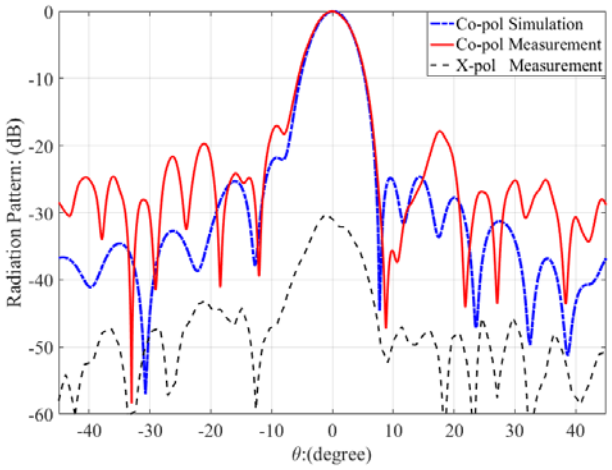

(a)

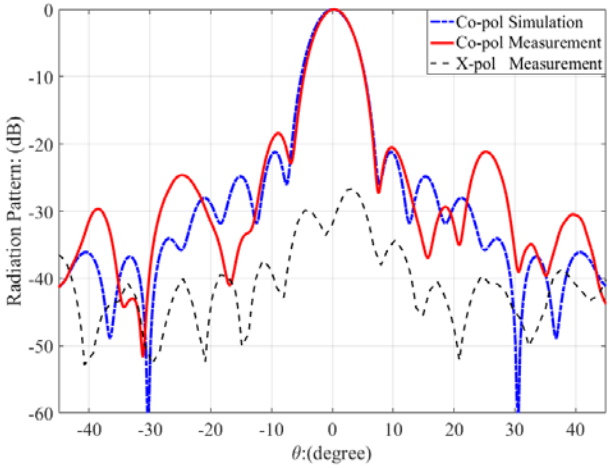

(b)

FIGURE 10. Calculated and measured radiation patterns: (a) E-plane, (b) H-plane.

TABLE 1. Comparison of the proposed antenna with existing designs.

Ref.	Freq. (GHz)	Simu. Gain (dB)	Meas. Gain (dB)	Meas. Aper. Efficiency	Opti. Blockage (%)	with Solar Cell	Weight
[21]	8.5	N/A	N/A	10%	N/A	Yes	Light
[24]	20	28.3	26.3	29.8%	17.6	Yes	Light
[25]	8.47	24.14	N/A	N/A	94.5	Yes	Light
[26]	8.47	26	N/A	N/A	94.6	Yes	Light
[29]	26	22.9	22.2	44.3%	~0	No	Light
[30]	11.7	26.7	26.16	25%	~0	Yes	Bulky
This work	20	28.4	27.3	40.0%	9.9	Yes	Light

The proposed reflectarray is compared with some of the existing designs in literature, and their performances are summarized in Table 1. The initial design in [21] realized an aperture efficiency of 10%, which was improved to be 29.8% with the tested gain of 26.3 dB at 20 GHz in [24]. Optimized optical transparency of 94.5% and better simulation results were reported in [25] and [26] with the gain of 26 dBi and aperture efficiency of 45%. Based on ITO material, transparent reflectarray without solar cell was investigated in [29] with the measured aperture efficiency of 44.3% and gain of 22.2 dBi. Another kind of transparent reflectarray was presented in [30]. The tested aperture efficiency was 25% with the tested gain of 26.16 dBi, almost no optical blockage exists at the expense of a bulky structure. The measured aperture efficiency is 40.0%, which is the highest measured result with solar cells. The optical blockage ratio in this work is 9.9%, significantly lower than that in [24], hence its impact on the solar cells is acceptable. Therefore, the proposed design can offer better radiation performances and a light structure.

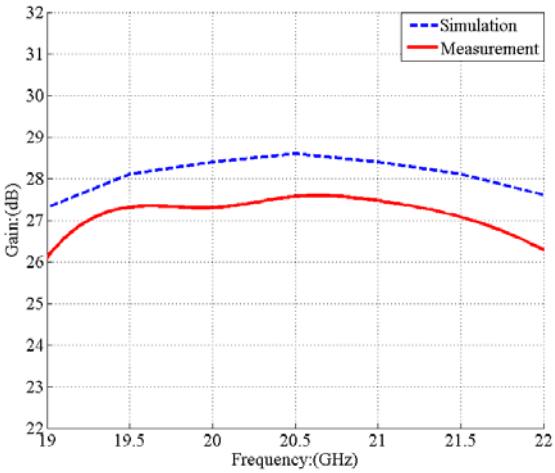

FIGURE 11. Calculated and measured gains within the frequency band of interest.

C. LIGHT TRANSMITTANCE EXPERIMENTAL RESULTS

For a multifunctional component, after successfully integrating the reflectarray on the surface of solar cells, it is also necessary to investigate the influence of reflectarray antenna on the solar energy harvesting. An experiment scenario is constructed to test the light transmittance at different circumstances with and without the X-dipoles printed on the top of coverglass for the proposed multiple functional design.

The calculation principle is derived from [24]. The output power of the solar cell (P_{out}) and its solar energy efficiency (η) are in linear relationship at the same incident optical power (P_{in}) in (2). From (2), the light transmittance can be deduced to be the ratio of the solar energy efficiencies with and without X-dipoles illuminated by a fixed optical source. Based on the analysis above, the light transmittance can be obtained only from the output powers of the solar cell while neglecting the incident optical power.

$$P_{\text{out}} = P_{\text{in}} \times \eta$$
$$\text{Transmittance} = \frac{P_{\text{out w/ X-dipoles}}}{P_{\text{out w/o X-dipoles}}} = \frac{\eta_{\text{w/ X-dipoles}}}{\eta_{\text{w/o X-dipoles}}} \quad (2)$$

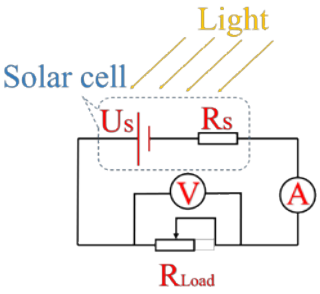

FIGURE 12. Equivalent circuit of the light transmittance experiment setup.

The experiment setup for measurements of light transmittance is similar to that in [24]. The corresponding equivalent circuit is depicted in Fig. 12. The entire experiment is conducted in a darkroom and a 45-W fluorescent lamp is chosen to be the equivalent optical source. The power source can be equalized to be serial connection of an ideal voltage source and a resistor. It is connected to a resistor load changing from 10 Ohm to 2750 Ohm. An ammeter and a voltmeter are utilized to measure the current and voltage of the resistor load.

The light transmittance of the solar cell is discussed for three cases: 1) a solar cell without coverglass; 2) a solar cell with coverglass only (without X-dipoles on it); and 3) a solar cell with coverglass and integrated X-dipoles. In order to compare the solar cell's responses under different illumination intensity, the distance between the lamp and the solar cell is chosen to be 25 mm and 50 mm, respectively. The current and voltage of the resistor load are measured at different circumstances for output power calculation, which is plotted in Fig. 13. It is observed that the output power becomes lower when increasing the separation distance, due to a reduced illumination power density. The coverglass and the X-dipoles continue to decrease the output power because of an increased optical blockage.

Based on the calculated output powers, the light transmittance can be derived, which is also plotted in Fig. 13. It is clear that the transmittances at two separation distance are all above 81%. After the output power peaking, the light transmittance begins to rise up to above 90% while the output power starts to decrease. The average transmittance is calculated to be 94.1% and 93.1% at the separation distance of 25 mm and 50 mm, respectively. Compared with the solar reflectarray in [24], the proposed design successfully decreases the optical blockage from 17.6% to 9.9% and increases the light transmittance from 64% to 81% at the point of maximum output power, which significantly improve the solar cell performance.

D. SUMMARIZED DESIGN GUIDELINE

The design guide lines for solar reflectarray are summarized as follows:

Firstly, the electromagnetic characteristics of the solar cell are investigated, including the conductivity, relative permittivity and loss tangent;

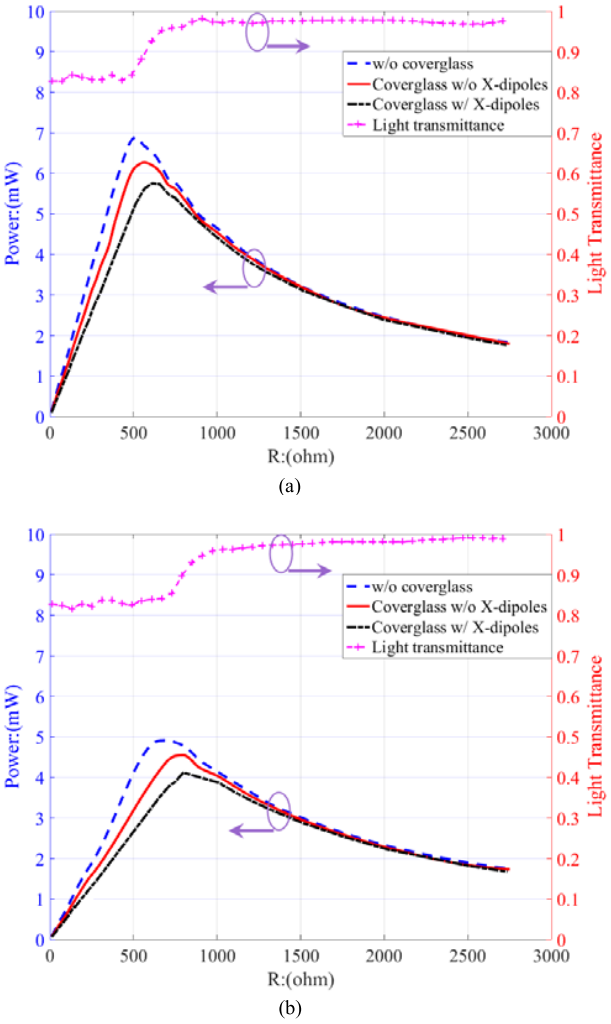

FIGURE 13. Calculated output power and light transmittance with different separation distance: (a) 25 mm, (b) 50 mm.

Secondly, the element structure is designed with less optical blockage and its performance is analyzed including the phase range of ∼360 degrees and less magnitude loss at normal incidence, the influence of the loss epitaxial layer and grid electrodes, the effect of oblique incidence on the element performance;

Thirdly, the array design is conducted with the modeling of the feed's radiation pattern, the feed position and main beam direction to avoid the feed blockage, phase distribution and magnitude distribution using ray tracing method, antenna array performance calculations (gains, efficiency and radiation pattern);

Lastly, optical experiment is performed.

IV. CONCLUSION

A Ka-band transparent reflectarray integrated with solar cells is designed and tested. The sub-wavelength X-shaped element has the ability of less magnitude loss and tolerating more phase errors. The measured array gain is 27.3 dBi with

an aperture efficiency of 40.0%, and the 1-dB gain bandwidth is 12.9%. Meanwhile the optical blockage ratio is reduced to be 9.9%. Solar transmittance experiment has been performed and the light transmittance is raised to be above 81%. Compared with previous designs, this work significantly improves the radiation performance of the reflectarray integrated with solar cells, and the solar harvesting performance at optical region. As an effective approach to reduce the volume and mass of major satellite components, the proposed high-gain antenna should find wide applications in future space communication systems.

ACKNOWLEDGMENT

The authors would like to thank the colleagues from the 41st Institute of China Electronics Technology Group Corporation for measuring the electromagnetic parameters of the glass glue.

REFERENCES

[1] M. Tanaka, R. Suzuki, Y. Suzuki, and K. Araki, "Microstrip antenna with solar cells for microsatellites," in *Antennas Propag. Soc. Int. Symp. (AP-S) Dig.*, vol. 2, Jun. 1994, pp. 786–789.
[2] S. V. Shynu, M. J. R. Ons, P. McEvoy, M. J. Ammann, S. J. McCormack, and B. Norton, "Integration of microstrip patch antenna with polycrystalline silicon solar cell," *IEEE Trans. Antennas Propag.*, vol. 57, no. 12, pp. 3969–3972, Dec. 2009.
[3] T. W. Turpin and R. Baktur, "Meshed patch antennas integrated on solar cells," *IEEE Antennas Wireless Propag. Lett.*, vol. 8, no. , pp. 693–696, 2009.
[4] M. J. Roo-Ons, S. V. Shynu, M. J. Ammann, S. J. McCormack, and B. Norton, "Transparent patch antenna on a-Si thin-film glass solar module," *Electron. Lett.*, vol. 47, no. 2, pp. 85–86, Jan. 2011.
[5] T. Wu, R. Li, and M. M. Tentzeris, "A scalable solar antenna for autonomous integrated wireless sensor nodes," *IEEE Antennas Wireless Propag. Lett.*, vol. 10, pp. 510–513, 2011.
[6] O. O'Conchubhair, P. McEvoy, and M. J. Ammann, "Dye-sensitized solar cell antenna," *IEEE Antennas Wireless Propag. Lett.*, vol. 16, pp. 352–355, 2017.
[7] O. O'Conchubhair, A. Narbudowicz, P. McEvoy, and M. J. Ammann, "Circularly polarised solar antenna for airborne communication nodes," *Electron. Lett.*, vol. 51, no. 9, pp. 667–669, 2015.
[8] O. Yurduseven and D. Smith, "A solar cell stacked multi-slot quad-band PIFA for GSM, WLAN and WiMAX networks," *IEEE Microw. Wireless Compon. Lett.*, vol. 23, no. 6, pp. 285–287, Jun. 2013.
[9] O. O'Conchubhair, P. McEvoy, and M. J. Ammann, "Integration of antenna array with multicrystalline silicon solar cell," *IEEE Antennas Wireless Propag. Lett.*, vol. 14, pp. 1231–1234, 2015.
[10] R. Caso, A. D'Alessandro, A. Michel, and P. Nepa, "Integration of slot antennas in commercial photovoltaic panels for stand-alone communication systems," *IEEE Trans. Antennas Propag.*, vol. 61, no. 1, pp. 62–69, Jan. 2013.
[11] S. Vaccaro, C. Pereira, J. R. Mosig, and P. D. Maagt, "In-flight experiment for combined planar antennas and solar cells (SOLANT)," *IET Microw., Antennas Propag.*, vol. 3, no. 8, pp. 1279–1287, Dec. 2009.
[12] S. V. Shynu, M. J. R. Ons, M. J. Ammann, B. Norton, and S. McCormack, "Dual band a-Si:H solar-slot antenna for 2.4/5.2 GHz WLAN applications," in *Proc. 3rd Eur. Conf. Antennas Propag.*, Mar. 2009, pp. 408–410.
[13] E. H. Lim and K. W. Leung, "Transparent dielectric resonator antennas for optical applications," *IEEE Trans. Antennas Propag.*, vol. 58, no. 4, pp. 1054–1059, Apr. 2010.
[14] A. Rashidian, L. Shafai, and C. Shafai, "Miniaturized transparent metallodielectric resonator antennas integrated with amorphous silicon solar cells," *IEEE Trans. Antennas Propag.*, vol. 65, no. 5, pp. 2265–2275, May 2017.
[15] O. O'Conchubhair, K. Yang, P. McEvoy, and M. J. Ammann, "Amorphous silicon solar Vivaldi antenna," *IEEE Antennas Wireless Propag. Lett.*, vol. 15, pp. 893–896, 2016.
[16] S. X. Ta, J. J. Lee, and I. Park, "Solar-cell metasurface-integrated circularly polarized antenna with 100% insolation," *IEEE Antennas Wireless Propag. Lett.*, vol. 16, pp. 2675–2678, 2017.
[17] S. Lemey, F. Declercq, and H. Rogier, "Dual-band substrate integrated waveguide textile antenna with integrated solar harvester," *IEEE Antennas Wireless Propag. Lett.*, vol. 13, pp. 269–272, Jan. 2014.
[18] E. H. Lim, K. W. Leung, C. C. Su, and H. Y, Wong, "Green antenna for solar energy collection," *IEEE Antennas Wireless Propag. Lett.*, vol. 9, pp. 689–692, 2008.
[19] J. Huang, "Capabilities of printed reflectarray antennas," *IEEE Phased Array Syst. Technol. Symp.*, Boston, MA, USA, Oct. 1996, pp. 131–134.
[20] M. Zawadzki and J. Huang, "Integrated RF antenna and solar array for spacecraft application," in *Proc. IEEE Int. Conf. Phased Array Syst. Technol.*, Dana Point, CA, USA, May 2000, pp. 239–242.
[21] J. Huang and M. Zawadzki, "Antennas integrated with solar arrays for space vehicle applications," in *Proc. ISAPE*, 2000, pp. 86–89.
[22] *Integrated Solar Array and Reflectarray Antenna (ISARA)*. [Online]. Available: http://www.nasa.gov/directorates/spacetech/small_spacecraft/isara_project.html
[23] T. Yekan, R. Baktur, and C. Swenson, "Examination of two types of quasi transparent reflectarray elements," in *Proc. IEEE Int. Symp. Antennas Propag. (APSURSI)*, Jun./Jul. 2016, pp. 1543–1544.
[24] W. An, S. Xu, F. Yang, and J. Gao, "A Ka-band reflectarray antenna integrated with solar cells," *IEEE Trans. Antennas Propag.*, vol. 62, no. 11, pp. 5539–5546, Nov. 2014.
[25] T. Yekan *et al.*, "Transparent reflectarray antenna printed on solar cells," in *Proc. IEEE 43rd Photovoltaic Spec. Conf. (PVSC)*, Jun. 2016, pp. 2610–2612.
[26] T. Yekan and R. Baktur, "Design of two transparent X band reflectarray antennas integrated on a satellite panel," in *Proc. IEEE Int. Symp. Antennas Propag. (APS-URSI)*, Jun./Jul. 2016, pp. 1413–1414.
[27] T. Yekan and R. Baktur, "Conformal integrated solar panel antennas: Two effective integration methods of antennas with solar cells," *IEEE Antennas Propag. Mag.*, vol. 59, no. 2, pp. 69–78, Apr. 2017.
[28] P. Dreyer, J. S. G. Díaz, and J. Perruisseau-Carrier, "Design of a reflectarray element integrated in a solar cell panel," in *Proc. IEEE Int. Symp. Antennas Propag.*, Jul. 2013, pp. 1558–1559.
[29] C. Kocia and S. V. Hum, "Design of an optically transparent reflectarray for solar applications using indium tin oxide," *IEEE Trans. Antennas Propag.*, vol. 64, no. 7, pp. 2884–2893, Jul. 2016.
[30] M. A. Moharram and A. A. Kishk, "Optically transparent reflectarray antenna design integrated with solar cells," *IEEE Trans. Antennas Propag.*, vol. 64, no. 5, pp. 1700–1712, May 2016.
[31] J. Ethier, M. R. Chaharmir, and J. Shaker, "Loss reduction in reflectarray designs using sub-wavelength coupled-resonant elements," *IEEE Trans. Antennas Propag.*, vol. 60, no. 11, pp. 5456–5459, Nov. 2012.
[32] F. Costa and A. Monorchio, "Closed-form analysis of reflection losses in microstrip reflectarray antennas," *IEEE Trans. Antennas Propag.*, vol. 60, no. 10, pp. 4650–4660, Oct. 2012.
[33] P. Nayeri, A. Z. Elsherbeni, and F. Yang, "Radiation analysis approaches for reflectarray antennas," *IEEE Antennas Propag. Mag.*, vol. 55, pp. 127–134, 2013.

WENXING AN received the B.S. and M.S. degrees from Zhengzhou University, Henan, China, in 2006 and 2009, respectively, and the Ph.D. degree from the Beijing University of Posts and Telecommunications, Beijing, China, in 2012, all in electrical engineering. From 2012 to 2014, he was a Post-Doctoral Research Engineer with the Department of Electronic Engineering, Tsinghua University, Beijing. From 2015 to 2016, he was a Research Fellow with the School of Electrical and Electronic Engineering, Nanyang Technological University, Singapore. In 2016, he has become an Associate Professor at the School of Microelectronic, Tianjin University, Tianjin, China. His research interests include dipole antennas, microstrip antennas, novel designs of reflectarray and transmitarray antennas, and circuits for advanced applications.

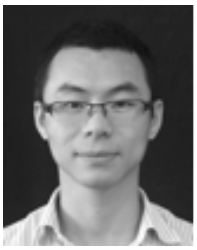

LIN XIONG received the B.S. degree in electrical engineering from the Central South University of Forestry and Technology, China, in 2006, and the M.S. degree in electrical engineering from the University of Electronic Science and Technology of China in 2013. In 2013, he became an Engineer with the Department of Electronic Engineering, Tsinghua University, Beijing, China. His research interests include the novel designs of reflectarray antennas for advanced applications and microwave devices.

SHENHENG XU (M'09) received the B.S. and M.S. degrees from Southeast University, Nanjing, China, in 2001 and 2004, respectively, and the Ph.D. degree from the University of California at Los Angeles (UCLA), Los Angeles, CA, USA, in 2009, all in electrical engineering. From 2000 to 2004, he was a Research Assistant with the State Key Laboratory of Millimeter Waves, Southeast University. Since 2004, he has been a Graduate Student Researcher and later a Post-Doctoral Researcher with the Antenna Research, Analysis, and Measurement Laboratory, UCLA. In 2012, he became an Associate Professor with the Department of Electronic Engineering, Tsinghua University, Beijing, China. His research interests include the novel designs of reflector and reflectarray antennas for advanced applications, evolutionary algorithms, and electromagnetic and antenna theories.

FAN YANG (S'96–M'03–SM'08) received the B.S. and M.S. degrees from Tsinghua University, Beijing, China, in 1997 and 1999, respectively, and the Ph.D. degree from the University of California at Los Angeles (UCLA), Los Angeles, CA, USA, in 2002.

From 1994 to 1999, he was a Research Assistant with the State Key Laboratory of Microwave and Digital Communications, Tsinghua University. From 1999 to 2002, he was a Graduate Student Researcher with the Antenna Laboratory, UCLA. From 2002 to 2004, he was a Post-Doctoral Research Engineer and an Instructor with the Electrical Engineering Department, UCLA. In 2004, he joined the University of Mississippi, Oxford, MS, USA, as an Assistant Professor, and then became an Associate Professor. Since 2010, he has been a Professor with Tsinghua University, and then the Director of the Microwave and Antenna Institute. He has authored or co-authored over 200 journal articles and conference papers, five book chapters, and three books *Electromagnetics and Antenna Optimization Using Taguchi's Method* (Morgan & Claypool, 2007), *Electromagnetic Band Gap Structures in Antenna Engineering* (Cambridge University Press, 2009), and *Scattering Analysis of Periodic Structures Using Finite-Difference Time-Domain Method* (Morgan & Claypool, 2012). His current research interests include antenna theory, electromagnetic band gap structures and their applications, computational electromagnetics, and applied electromagnetic systems.

Dr. Yang was a recipient of the several prestigious awards and recognitions, including the 2004 Certificate for Exceptional Accomplishment in Research and Professional Development Award from UCLA, the Young Scientist Award from the 2005 URSI General Assembly and from the 2007 International Symposium on Electromagnetic Theory, the 2008 Junior Faculty Research Award from the University of Mississippi, the 2009 inaugural IEEE Donald G. Dudley Jr. Undergraduate Teaching Award, and the 2011 Global Experts Program of China. He was the TPC Chair of the 2014 IEEE AP-S International Symposium. He is also a frequent reviewer for over 20 scientific journals and book publishers. He has chaired numerous technical sessions in various international symposia. He was an Associate Editor of the IEEE TRANSACTIONS ON ANTENNAS AND PROPAGATION and *Applied Computational Electromagnetics Society Journal*.

HAI-PENG FU (S'06–M'12) received the B.S. degree in communication engineering from the Harbin Institute of Technology, Harbin, China, in 2003, the M.S. degree from the Royal Institute of Technology, Stockholm, Sweden, in 2010, and the Ph.D. degree in electrical engineering from Fudan University, Shanghai, China, in 2012. He is currently a Lecturer with the School of Electronic Information Engineering, Tianjin University, Tianjin, China. His current research interests include RF integrated circuits and RF integrated systems for wireless, microwave device characterization modeling, monolithic microwave integrated circuits, and reliability physics modeling of electronic components and systems.

JIAN-GUO MA (SM'97–F'16) received the B.Sc. degree from Lanzhou University, Lanzhou, China, in 1982, and the Ph.D. degree in engineering from the University of Duisburg-Essen, Duisburg, Germany, in 1996. He was with the Technical University of Nova Scotia, Halifax, NS, Canada, as a Post-Doctoral Fellow, from 1996 to 1997. From 1997 to 2005, he was with Nanyang Technological University (NTU), Singapore, as a Faculty Member, where he was also the Founding Director with the Center for Integrated Circuits and Systems, NTU. From 2005 to 2009, he was with the University of Electronic Science and Technology of China, Chengdu, China. Since 2008, he has been the Technical Director with the Tianjin Integrated Circuit Design Center, Tianjin University. Since 2009, he has been the Dean of the School of Electronic Information Engineering, Tianjin University. His current research interests include RF integrated circuits and RF integrated systems for wireless, RF device characterization and modeling, and microwave and terahertz microelectronic systems. He is a member of the Editorial Board of the PROCEEDINGS OF THE IEEE and a member of the IEEE University Program Ad Hoc Committee from 2010 to 2013. He was a recipient of the Changjiang Professor of the Ministry of Education of China. He was also a recipient of the Distinguished Young Investigator Award of the National Natural Science Foundation of China. He was an Associate Editor of the IEEE MICROWAVE AND WIRELESS COMPONENTS LETTERS from 2003 to 2005.